PASSIVE HEATING AND COOLING IN A BUILDING WITH A SOLAR AIR HEATER AND ITS THERMAL PERFORMANCE WITH 3/4 RHOMBUS ROUGHNESS

Ravi Kumar Research Scholar, Aryabhatta Knowledge University-Bihar
Nivedan Mahato Assistant Professor, ARKA JAIN University-Jharkhand
K.N. Prasad Principal,Govt Engineering college, Banka
Manikant Paswan Professor, NIT Jamshedpur

Abstract

Solar air heaters have been used for many applications requiring low to medium grade thermal energy, like, space heating and cooling, agricultural drying, timber seasoning, mainly due to their low manufacturing cost, simple design, operating and maintenance. Several designs for the enhancement of heat transfer coefficient and hence the improvement of thermal performance of solar air heaters have been proposed and investigated by a number of investigators. Such designs are honeycomb collector, corrugated absorber, V- shape absorber, extended surfaces absorber, double-exposure collector, two pass collector, packing of porous material in air flow channel i.e. packed bed absorbers and use of artificial roughness on the absorber plate. The artificial roughness has been used as an effective means for improvement of thermal performance of solar air heaters. However, this result in increase in friction factor for fluid flow. A number of investigators have studied the phenomenon of heat transfer enhancement in solar air heater duct in form of small diameter wire, expanded metal foil, wire screen metal mesh, at the bottom side of absorber plate. However, literature is incomplete for use of rhombus shape as a turbulent promoter in solar air heaters.

Introduction

Among solar collectors, solar air heaters occupy an important place. Solar air heaters are mainly used for drying or curing agricultural products, heating space for comfort, wood seasoning, and curing industrial products such as plastic. Cheaper and easier to install than other solar collectors. In general, solar air heaters are well suited for low and medium temperature applications because their design is relatively simple. However, its usefulness as an energy harvesting device is limited by its low thermal efficiency, mainly due to the low convective heat transfer coefficient between the absorber plate and the flowing air, leading to high plate temperature and heat loss. Several methods have been proposed by researchers to improve the thermal efficiency of solar air heaters.

Therefore, the most acceptable method is to use artificial roughness with different shape and size on the absorber plate. By providing artificial roughness, the thermal efficiency of a solar air heater can be improved. With a roughened surface, we can increase the heat transfer coefficient, so that turbulence can arise. In order to achieve the maximum heat transfer coefficient, turbulence must be created near the surface of the absorber plate. Thus, the most promising technique for creating turbulence is to create an artificial roughness on the absorber plate. One of the effective methods to increase the heat transfer rate and increase the turbulence inside the channel using half diamond surfaces.

In this chapter the parametric analysis has been carried out analytically to investigate the performance of solar air heater using half rhombus absorber plate. Various parameters like temperatures, air velocity, and mass flow rate have been measured by different types of equipments. Here experiment performed at different temperatures at inlet and outlet section and thermocouples have been used at different positions for measuring the temperature at different locations. The characteristics of solar air heater have been performed at different mass flow rate. The experiment has performed between two kinds of ducts, one is smooth absorber plate and other is roughened absorber plate. In this study, it is found that the maximum heat transfer occurred at roughened absorber plate as compared to smooth absorber plate. The change in the mass flow rate appreciably affects the performance because the value of the air side heat transfer coefficient is relatively low. So in order to obtain complete information on a solar air heater, it becomes necessary to conduct tests over a range of mass flow rates with each flow rate yielding its own efficiency curve.

The pictorial view of absorber plate with artificial roughness of half rhombus shape is given below in figure 1. This absorber plate is of galvanized iron (GI) having thickness of 0.8 mm. wires are attached on absorber plate in half rhombus shape. The material for wire is aluminum wire of diameter 2 mm. The length and width of absorber plate are 1400 mm and 330 mm respectively.

Fig. 1. : Pictorial view of Artificial Roughness with shape of 3/4th rhombus.

EXPERIMENTAL PROCEDURE

The assembly was mounted on wooden stands such that the suction side of the blower is aligned with the pipe connected to the air heaters and flow strengtherners in horizontal position as shown in Fig 3.1. All the components of the set-up were cheked for their positioning so that the collector covers and absorbers are in a horizontal position. The joints between the entry and exit sections as also the other points of possible leakage were properly sealed. All the thermocouples were tested for their correctness while in situ. Precaution was taken so that connector was not exposed to direct solar radiation which might lead to erroneous results. All other measuring instruments i.e. orifice meter microvoltmenter, U-tube manometer were properly checked.

The collectors were tested in a horizontal position using an open-loop flow system proposed in ASHRAE 93-97 [64]. Tests were conducted under controlled conditions of mass flow rate (i.e. flow Reynolds number) and the roughness parameters (p/de, de/D_h) and under outdoor conditions with varying values of solar radiation intensity and ambient temperature. Test data were collected at hourly (half hourly in some cases) intervals each day between 10.00 AM to 2.00 PM in the month of Feb 2022 to June 2022. The following parameters were measured.

i) Pressure difference across orificemeter.
ii) Pressure drop across the duct.
iii) Temperature of the absorber plate
iv) Temperature of air in the duct.
v) Ambient temperature.
vi) Intensity of solar radiation.

In 240 number of runs, 5 set of roughened absorber plate, each under six values of flow rates were tested (Table 3.1)

Table 1: Range of Parameters Investigated, prandtle number (air at average temperature) of 0.7

Set No.	Un No.	Date	Re	m kg/s	p mm	de mm	p/de	de/dh
1	2	3	4	5	6	7	8	9
1	1	26.2.2022	3000-8000	0.033	3.412	0.412	8.28	0.0141
	2	29.2.2022		0.044				
	3	3.2.2022		0.05				
	4	4.2.2022		0.053				
	5	5.2.2022		0.058				
	6	5.2.2022		0.067				
2	7	10.3.2022	3500-8500	0.033	3.312	0.41	8.07	0.0137
	8	12.3.2022		0.044				
	9	15.3.2022		0.05				
	10	17.3.2022		0.053				

	11	19.3.2022		0.058				
	12	22.3.2022		0.067				
3	13	25.3.2022	3500-8500	0.033	3.312	0.41	5	0.0137
	14	28.3.2022		0.044				
	15	31.3.2022		0.05				
	16	2.4.2022		0.053				
	17	4.4.2022		0.058				
	18	7.4.2022		0.067				
4	19	9.4.2022	3500-8500	0.033	2.208	0.508	4.34	0.0137
	20	11.4.2022		0.044				
	21	14.4.2022		0.05				
	22	17.4.2022		0.053				
	23	19.4.2022		0.058				
	24	21.4.2022		0.067				
5	25	23.4.2022	3500-8500	0.033	1.814	0.508	3.58	0.0137
	26	26.4.2022		0.044				
	27	28.4.2022		0.05				
	28	30.4.2022		0.053				
	29	2.5.2022		0.058				
	30	5.5.2022		0.067				
6	31	8.5.2022	3500-8500	0.033	4.618	0.508	8.87	0.0137
	32	10.5.2022		0.044				
	33	12.5.2022		0.05				
	34	15.5.2022		0.053				
	35	17.5.2022		0.058				
	36	19.5.2022		0.067				
7	37	22.5.2022	3500-8500	0.033	3.175	0.508	6.24	0.0137
	38	24.5.2022		0.044				
	39	26.5.2022		0.05				
	40	27.5.2022		0.053				
	41	29.5.2022		0.058				
	42	30.5.2022		0.067				
8	43	1.6.2022	3500-8500	0.033	2.54	2.54	5	0.0137
	44	2.6.2022		0.044				
	45	3.6.2022		0.05				
	46	5.6.2022		0.053				
	47	6.6.2022		0.058				
	48	7.6.2022		0.067				
9	49	8.6.2022	3500-8500	0.033	2.208	2.208	4.34	0.0137
	50	9.6.2022		0.044				
	51	10.6.2022		0.05				
	52	12.6.2022		0.053				
	53	13.6.2022		0.058				
	54	14.6.2022		0.067				
10	55	15.6.2022	3500-8500	0.033	1.814	1.814	3.58	0.0137
	56	16.6.2022		0.044				
	57	18.6.2022		0.05				
	58	19.6.2022		0.053				
	59	20.6.2022		0.058				
	60	21.6.2022		0.067				

EXPERIMENTAL DATA

The raw experimental data during experimentation which included thermocouples reading, air mass flow rates, pressure drop in ducts, ambient temperature and intensity of solar radiation had been tabulated. Table 3.1 shows the data collected during a typical run for a particular set.

Table 2 Thermocouple Reading $°c$

		t1	t2	t3	t4	t5	t6	t7	t8	t9	t10	t11	t12
1	R	33.4	34.8	34.9	34.9	35.3	35.2	38.8	35.9	35.8	39.9	40.2	40.4
	S	32.6	33.6	33.8	33.8	34.2	34.3	34.6	34.7	34.3	37.3	37.3	37.4
2	R	34.3	34.7	34.9	35.2	35.3	35.5	35.5	34.9	35.8	39.9	40.4	40.6
	S	33.6	33.8	33.8	34.1	34.3	34.3	34.5	34.6	34.9	37.8	38.8	38.3
3	R	34.5	34.9	35.1	35.3	35.3	35.5	35.6	35.8	35.9	37.2	40.9	41.2
	S	33.8	33.8	33.9	34.1	34.4	34.7	34.8	34.9	37.7	35.3	39.1	39.9
4	R	35.2	35.3	35.7	35.9	35.9	35.8	36.2	36.4	36.6	37.8	41.2	42.3
	S	34.3	34.4	34.8	34.7	34.8	34.9	34.9	34.7	34.9	35.7	39.1	39.7
5	R	35.9	35.9	36.2	36.4	36.8	36.9	37.2	37.4	37.2	37.9	42.3	42.8
	S	34.8	34.7	34.9	34.9	37.2	37.2	38.1	38.1	34.9	37.8	41.8	41.3

Table 3: I, t_a, Δ t and h as a function of time during the day (Room No. H.T. Lab)

Time AM/PM	10.00	11.00	12.00	1.00	2.00
I, mv	8.2	8.9	9.3	9.8	9.6
ta, °C	29.9	30.2	31.4	32.12	34.6
tr °C	38	40	43	45	46
TB,°C	39	41	43.5	45.6	45.6
h w/m2k	19.7	20.5	20.8	20.9	21.6
Nu	34.2	35.6	35.9	36.2	36.3
hs w/m2	18.3	18.4	18.6	18.8	18.8
Nus	23.2	23.1	23.2	23.2	23.2

Results and Discussion

Altogether in 45 number of test runs, raw experimental data were collected for 05 set of roughened solar air heaters, simultaneously with the smooth ones. For a particular test run, mass flow rate in the roughened and smooth collector remained the same.

The value of the hydraulic diameter D of the solar air heater ducts (both smooth and roughened) has been worked out to be 0.042 m.

The raw experimental data were reduced to work out for the values of the results with respect to heat transfer which have been represented through the different Tables and figures as follows:

4.1 Heat Transfer

Fig 4.1, 4.2, 4.3, 4.4, 4.5 and 4.6 represents the heat transfer results in the form of Nusselt number for smooth and roughened collectors. The analytical and experimental values of Nusselt number for smooth and roughened collectors have been compared. The analytical values of Nusselt number have been worked out using the following Eqs. (1) and (2) from reference Prasad and Saini (1988):

$$Nu_s = 0.0158Re^{0.8} \qquad (4.1.1)$$

$$\overline{Nu_r} = \frac{\left(f/_2\right)Re^{0.9}Pr^{0.5}}{1+\sqrt{f/_2}\left[4.5(e^{+})^{0.28}Pr^{0.57}-0.95\left(P/_e\right)^{0.53}\right]} \qquad (4.1.2)$$

Where, $e^{+} = e/_D\left(\sqrt{f/_2}\right)Re$ (4.1.3)

$$f= \frac{f_r+f_s}{2} \qquad (4.1.4)$$

and f_r has been taken from references Sheriff and Gumley(1966), Written as under:

$$f_r = \frac{2}{\left[0.95\left(P/_e\right)^{0.53}+2.5ln\left(D/_{2e}\right)-3.75\right]^2} \qquad (4.1.5)$$

The values of are taken from the Moody Chart.

The Experimental values of the heat transfer coefficient for smooth and roughened collectors have been found out from Eq. (4.6) as under:

$$\acute{m}C_p(t_0 - t_i) = hA_c(t_p - t_0) \tag{4.1.6}$$

Which have been further used to obtain the values of Nusselt number for smooth and roughened collectors from the following equation:

$$Nu = h\,D / k \tag{4.1.7}$$

Table 4.1	Heat transfer data for Roughened collector (P/e=40; e/D=0.071)					
Re	Tp	T0	Ti	ma	h	Nu_r
2077	65	42	31	0.02	21.66025	31.37002
4067	66	39	30	0.03	22.53772	32.64084
6078	66	40	30	0.035	29.05941	42.08604
7737	61	39	29	0.04	40.9199	59.2633
10080	62	39	28	0.045	48.43125	70.14

Table 4.2	Heat transfer data for Roughened collector (e/D=0.119; P/e=40)					
Re	Tp	T0	Ti	ma	h	Nu_r
2077	60	42	29	0.02	34.86384	50.49246
4067	60	42	28	0.03	52.55313	76.11142
6078	60	41	28	0.035	51.64911	74.80216
7737	59	40	28	0.04	56.84295	82.32427
10080	62	40	28	0.045	55.23421	79.99438

Table 4.3	Heat transfer data for Smooth collector					
Re	Tp	T0	Ti	ma	h	Nus
2077	60	34	29	0.02	9.283271	13.44474
4067	60	33	28	0.03	12.51265	18.12177
6078	60	33	28	0.035	13.9791	20.2456
7737	59	33	28	0.04	17.30795	25.06669
10080	59	33	27	0.045	23.35797	33.82878

Table 4.1 and 4.2 represents the raw data for heat transfer coefficient and Nusselt number for corresponding values of Different Reynolds numbers and for the particular value of relative roughness pitch (P/e) equals to 40 and relative roughness height (e/D) equals to 0.071 and relative roughness pitch (P/e) equals to 40 and relative roughness height (e/D) equals to 0.119, for roughened absorber plates respectively. Table 4.3 shows the same but for smooth absorber plate.

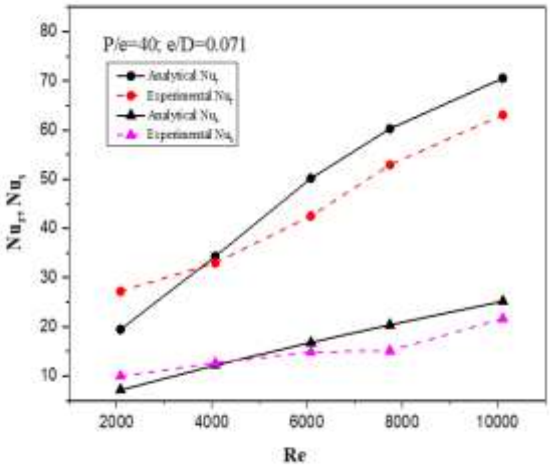

Fig. 4.1 Comparison of analytical and experimental heat transfer data

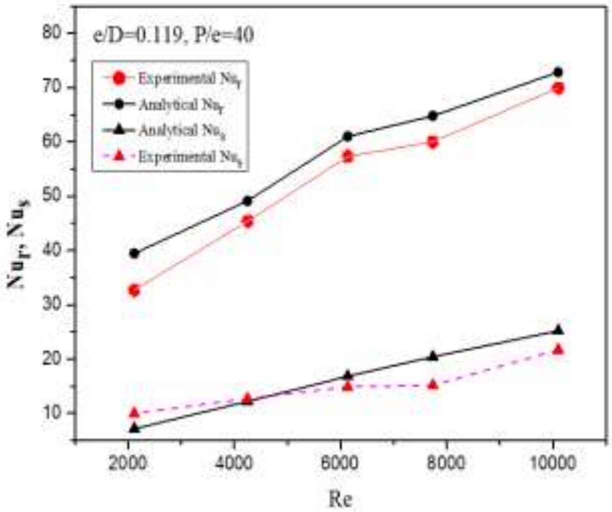

Fig. 4.6 Comparison of analytical and experimental heat transfer data

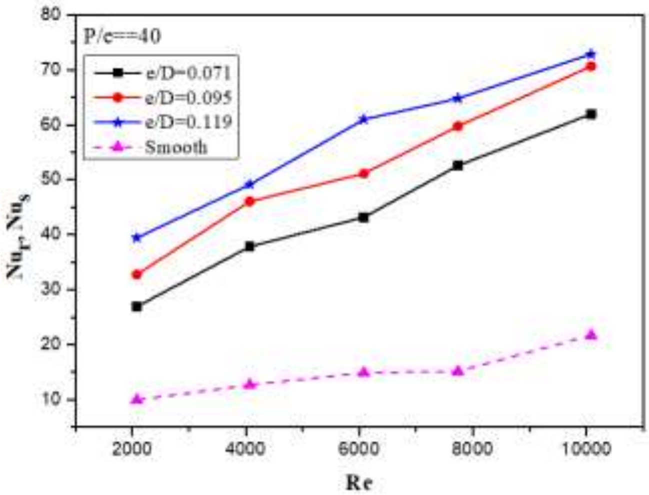

Fig. 4.8 Effect of e/D on heat transfer in artificially roughened solar air heater

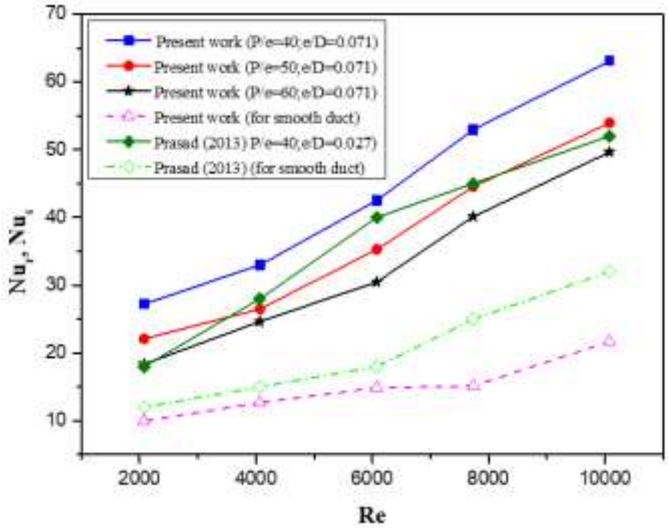

Fig. 4.9 Comparison of effect of P/e on heat transfer in artificially roughened solar air heater

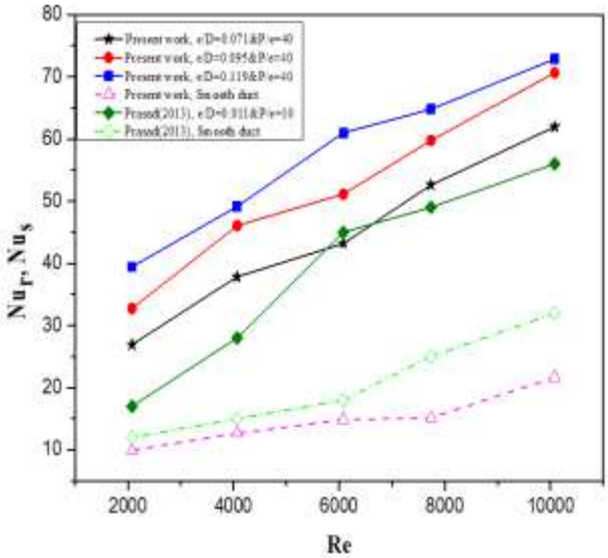

Fig. 4.10 Comparison of Effect of e/D on heat transfer in artificially roughened solar air heater

Fig. 4.1 represent typically the comparison of the experimental and analytical values of Nusselt number in smooth and roughened solar air heaters for a given value of relative roughness height (e/D) equal to 0.071 at values of relative roughness pitch(P/e) of 40. Fig. 4.8 represents the effect of relative roughness pitch (P/e) for a given value of relative roughness height (e/D) on heat transfer. The experimental and analytical values of Nusselt number compare well with a percentage mean deviation of +6.0, 7.0 and 7.2. For relative roughness pitch (P/e), equal to 40, 50 and 60 respectively for the flow Reynolds number varying from 2077 to 10080. The experimental and analytical values of Nusselt number compare well with a percentage mean deviation of +6.0, 7.0 and 7.2. For relative roughness pitch (P/e) equal to 40, 50 and 60 respectively which is +6.0 in case of smooth collector for the flow Reynolds number varying from 2077 to 10080. The Values of the mean deviation have been found out as under.

Deviation = (Experimental values - Analytical values) / Experimental values.

Within the range of the parameters investigated, percentage mean deviation between the experimental and analytical values of Nusselt number has been found in the range of -4% to +13.06% for the roughened collectors and -16.2% to +3.7% for the smooth collectors.

Now, that the experimentally and analytical results on the heat transfer have been found to compare reasonably well, Fig. 4.8 have been drawn typically to see the effect of roughness parameters relative roughness pitch (P/e) and relative roughness height (e/D) respectively, on Nusselt number in roughened collectors, as also to compare with the Nusselt number in those of the smooth collectors at the same values of flow Reynolds Number. It could be seen the effect of relative roughness height (e/D) for a given value of relative roughness pitch (P/e), that the value of Nusselt number increases with the increase in the value of relative roughness height (e/D). At a flow Reynolds number of 10080, the values of Nusselt number in rough collector are about 63.36, 72.83 and 74.08 for the respective values of relative roughness height (e/D) equals to 0.071, 0.095 and 0.119 at a given value of relative roughness pitch (P/e) equals to 40, whereas it is 21.7 in case of smooth collector.

Fig. 4.9 and 4.10 show the comparison of effect of relative roughness pitch (P/e) and effect of relative roughness height (e/D) on heat transfer of roughened solar air heater. Within the range of the parameters investigated, the value of the "Enhancement Factor (Nu_r/Nu_s)," has been found out to be in the range of 2.5 to 3.9, the higher values corresponding to the smaller value of relative roughness pitch (P/e) and higher values of relative roughness height (e/D). It is to mention that reattachment of free shear-layer with the surface is necessary for effective heat transfer from the surface, which may not occur for the value of P/e less than 40 As it becomes like smooth surface. For relative roughness pitch, P/e, value higher than 40, lesser number of roughness element (rhombus shape sheet) on the collector have a lesser effect of induced turbulence in the viscous sub- layer, resulting in reduction of heat transfer and hence lower the Nusselt number.

THERMAL PERFORMANCE

The solar air heaters, operating without recycling of air, thermal performance has been represented on the basis of outlet air temperature (Gupta and Garg, 1967). The following equations have formed the basis of representation of thermal efficiency:

$$\eta_{th} = F_R(\tau\alpha) - F_R U_L (t_0 - t_i)/I \quad (4.2.1)$$

$$\eta_{th} = \dot{m} C_p (t_0 - t_i)/I \quad (4.2.2)$$

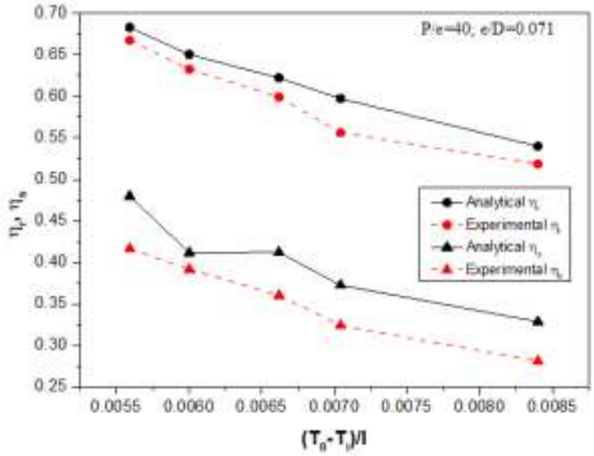

Fig. 4.11 Comparison of analytical and experimental thermal performance of roughened solar air heater at different relative roughness pitch (P/e)

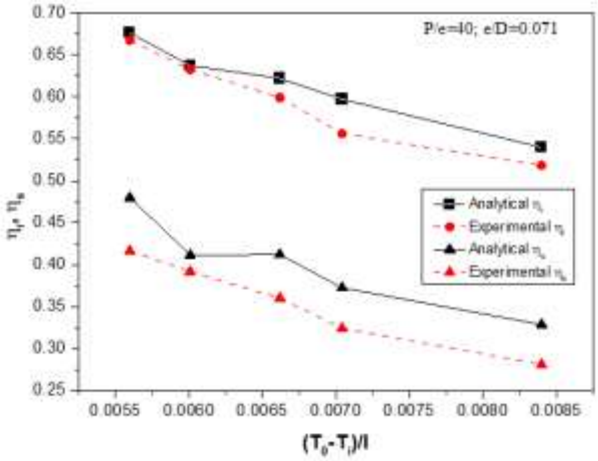

Fig. 4.14 Comparison of analytical and experimental thermal performance of roughened solar air heater at different relative roughness height (e/D)

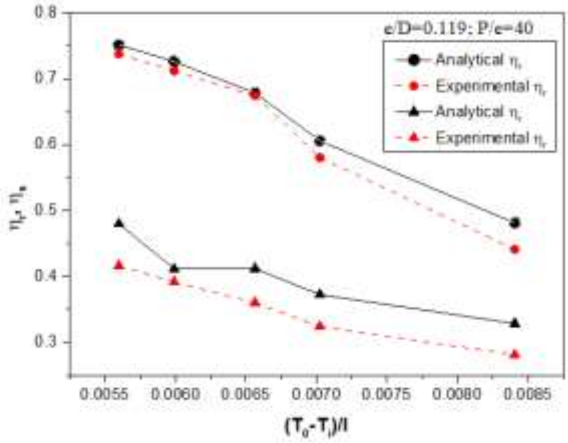

Fig. 4.16 Comparison of analytical and experimental thermal performance of roughened solar air heater at different relative roughness height (e/D)

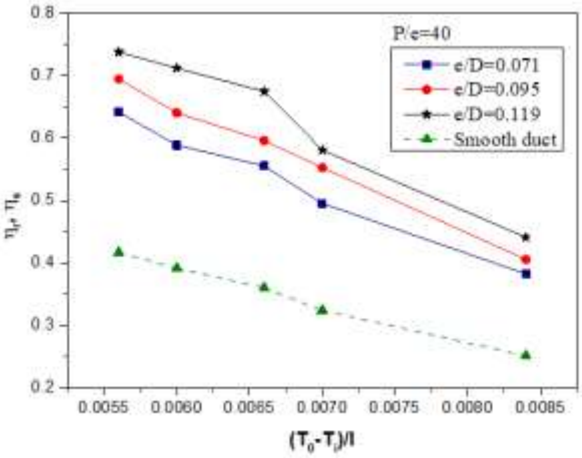

Fig. 4.18 Effect of relative roughness height (e/D) on performance of roughened solar air heater

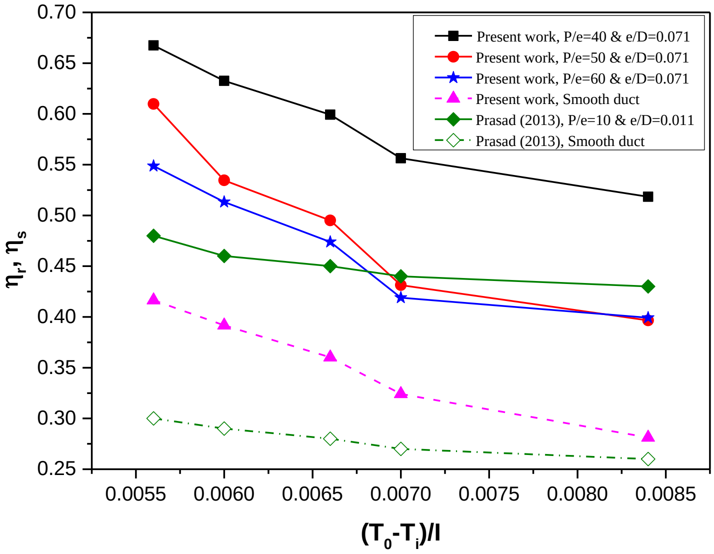

Fig. 4.19 Comparison of effect of relative roughness pitch (P/e) on performance of roughened solar air heater

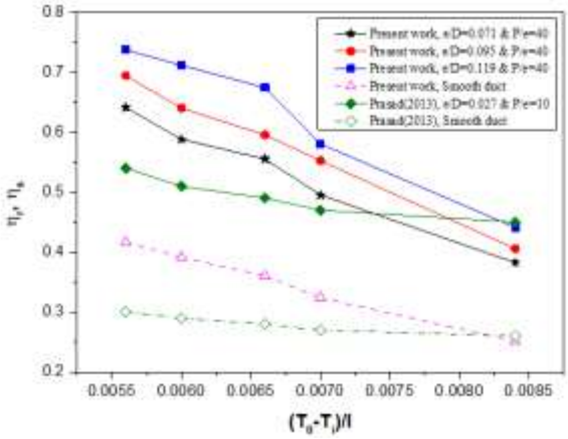

Fig. 4.20 Comparison of effect of relative roughness height (e/D) on performance of roughened solar air heater

The performance of solar air heaters is a strong function of mass flow rate, which necessitates that, in order to obtained a reasonably reliably information with regard to the thermal performance of solar air heaters, each mass flow rate results in a efficiency curve. Fig. 4.11 represent typically the analytical and experimental performance characteristic of the roughened collectors for relative roughness pitch (P/e) equals to 40' for a particular value of relative roughness height (e/D) equals to 0.071 and also for smooth collectors at various mass flow rates. Similarly, Fig. 4.14 represent typically the analytical and experimental performance characteristic of the roughened collectors for relative roughness height (e/D) equals to 0.071 for a particular value of relative roughness pitch (P/e) equals to 40 and also for smooth collectors at various mass flow rates.

It is obvious from Fig. 4.18 that for a given mass flow rate, the performance of roughened solar air heater increases with decreasing value of relative roughness pitch (P/e) and increasing value of relative roughness height (e/D). For instance, Fig.4.2.7 at a given mass flow rate m = 0.045 and relative roughness pitch (P/e), equals to 40 the values of thermal efficiency of roughened solar air heater are found to be about 66.7%, 69.4% and 73.7% for relative roughness height (e/D), equals to 0.071 respectively as compare to about 41.7% for that of smooth solar air heater. Similarly, in fig. 4.2.8 at a given mass flow rate m = 0.045 and relative roughness height (e/D), equals to 0.071 the values of thermal efficiency of roughened solar air heater are found to be about 67.7%, 60.9% and 52.5% for relative roughness pitch (P/e), equals to 40 respectively as compare to about 41.7% for that of smooth solar air heater. Fig. 4.19 and 4.20 show the comparison of effect of relative roughness pitch (P/e) and effect of relative roughness height (e/D) on performance of roughened solar air heater.

AVERAGE HOURLY VARIATION OF T_P , T_0 AND T_i

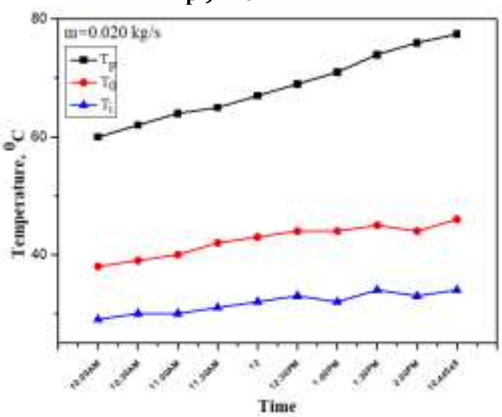

Fig. 4.35 Average hourly variation of T_P, T_0 and T_i

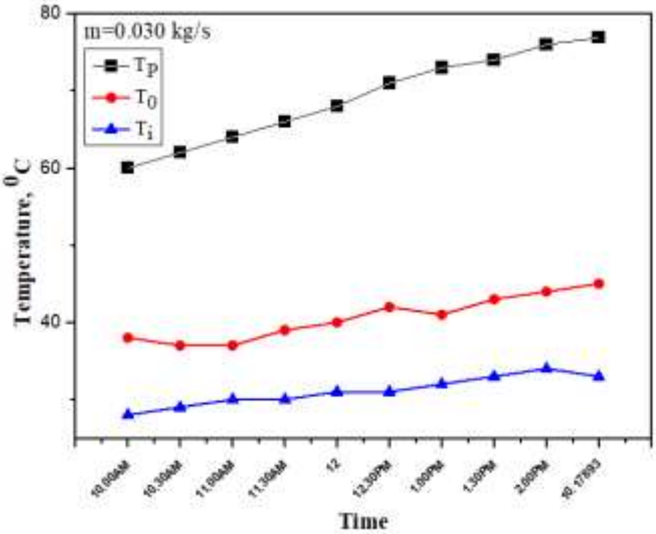

Fig. 4.36 **Average hourly variation of T_P, T_0 and T_i**

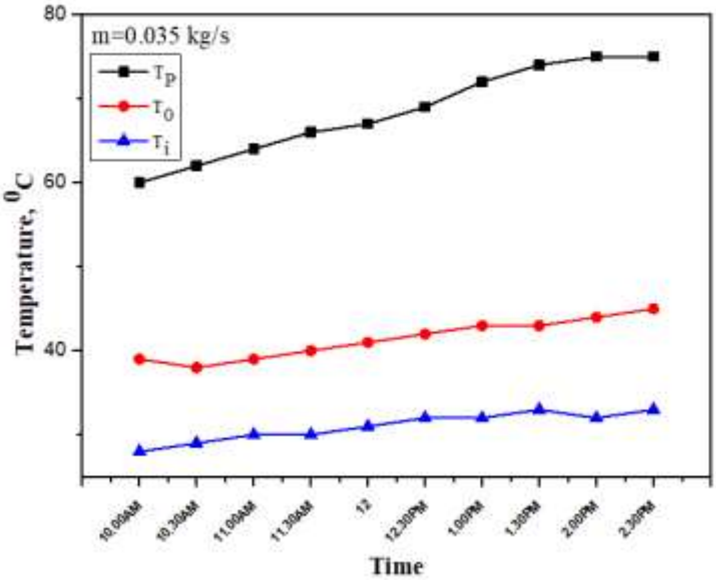

Fig. 4.37 **Average hourly variation of T_P, T_0 and T_i**

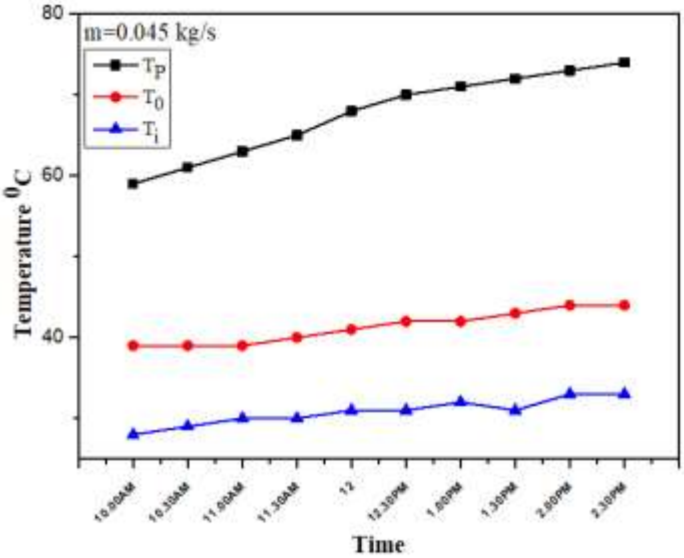

Fig. 4.38 **Average hourly variation of T_P, T_0 and T_i**

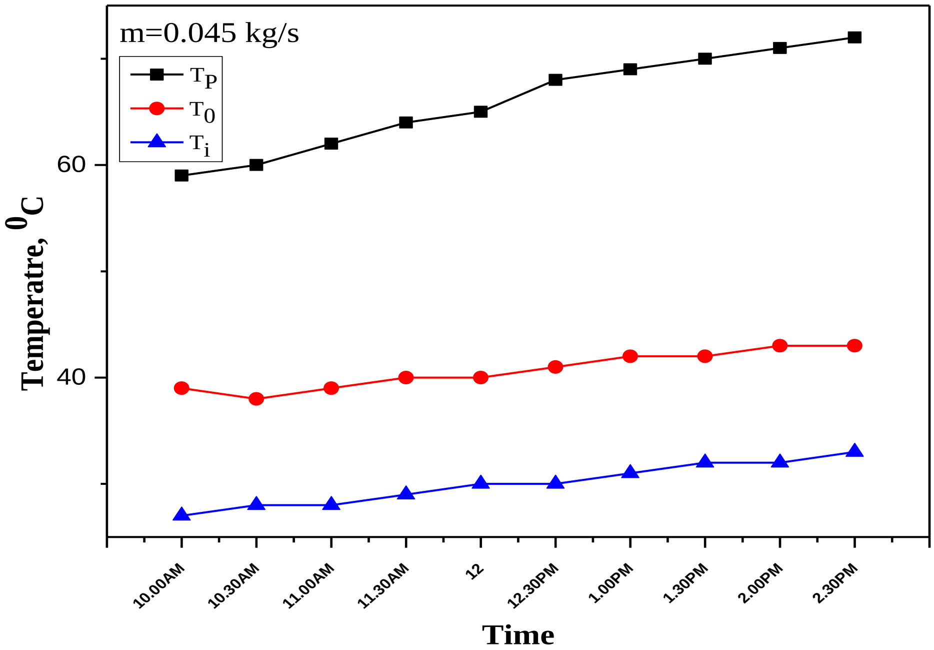

Fig. 4.39 Average hourly variation of T_P, T_0 and T_i

Fig. 4.35, 4.36, 4.37, 4.38 and 4.39 shows the values of hourly variation of average temperature of collector (T_P), average temperature of outlet air (T_0) and average temperature of inlet air (T_i) for different values of mass flow rate. The range of average temperature of collector (T_P), average temperature of outlet air (T_0) and average temperature of inlet air (T_i) have been found to be 60 to 78^0C, 38 to 46^0C and 29 to 34^0C for a particular value of mass flow rate, m, equals to 0.020 kg/s.

It is also seen from the figures that the average temperature of collector (T_P), average temperature of outlet air (T_0) and average temperature of inlet air (T_i) gets decreases as the value of mass flow rate increases.

CONCLUSION

Present investigation of rhombus shape roughened solar air heater has been proposed and used to predicts to heat transfer, thermal performance and friction factor with relative roughness pitch (P/e), relative roughness height (e/D) and Reynolds number. The following conclusions have been derived on the basis of the results and discussions:

1. The average Nusselt number tends to increase as the Reynolds number increases in all cases. The average Nusselt number tends to decrease as the relative roughness pitch (P/e) increases for a fixed value of relative roughness height (e/D) and it also tends to increases as the relative roughness height increases for a fixed value of relative roughness pitch.
2. The maximum enhancement in the Nusselt number has been found to be 3.89 times over the smooth duct corresponding to the relative roughness height (e/D) of 0.119 and relative roughness pitch (p/e) of 40 at Reynolds number of 10080 in the range of parameters investigated.
3. The maximum enhancement in the friction factor has been found to be 3.42 times over the smooth duct corresponding to the relative roughness height (e/D) of 0.119 and relative roughness pitch (P/e) of 40 at Reynolds number of 10080 in the range of parameters investigated.
4. The thermal efficiency of roughened solar air heaters increases with the increasing values of flow Reynolds number and relative roughness height for a given value of relative roughness pitch.

5. The thermal efficiency of the roughened solar air heaters increases with the increasing value flow Reynolds number and decreasing value of relative roughness pitch for a given value of relative roughness height.

[1] Gier JT and Dunkle R.V., 1958. Selective spectral characteristics as an important factor in the efficiency of solar collectors. Trans. Conf. on the use of Solar Energy 2(1), 41

[2] Government decides to electrify 5.98 crore unelectrified households by December 2018. (http://economictimes.indiatimes.com/industry/energy/ power/government decides-to-electrify-598-crore-un-electrified-households-by december 2018/article show/52825361.cms). Retrieved 20 December 2016

[3] Government working to double generation target from solar parks" (http://economictimes.indiatimes.com/industry/energy/power/governmentwork ing-to-double-generation-target-from-solar-parks/articleshow/53268569.cms). Economic Times. 18 July 2016. Retrieved 18 July 2016.

[4] Griggs E.I. and Sharifabad F.K., 1992. Flow characteristics in rectangular ducts. ASHRAE Trans 98(1), 116-27.

[5] Growth of Electricity Sector in India from 1947-2016" (http://www.cea.nic.in/reports/others/planning/pdm/growth_2016.pdf) (PDF). CEA. Retrieved 17 February 2017.

[6] Gupta D., Solanki S.C. and Saini J.S., 1997. Thermohydraulic performance of solar air heaters with roughened absorber plates. Solar Energy 61, 33-42

[7] Hahne E. Fisch N. and Arafa A., 1978 (June). The flat plate solar collector - its steady state transient state behaviour, Proc. Int. Symposium - Workshop on Solar Energy, 1, 159-186, Cairo, Egypt

[8] Handoyo E. A., Djatmiko Ichsani, Prabowo and Sutardi, 2014. Experimental Studies on a Solar Air Heater Having V-Corrugated Absorber Plate with Obstacles Bent Vertically. Applied Mechanics and Materials 493, 86 – 92

[9] Handoyo E. A., Djatmiko Ichsani, Prabowo and Sutardi, 2016. Numerical studies on the effect of delta-shaped obstacles spacing on the heat transfer and pressure drop in v-corrugated channel of solar air heater. Solar Energy 131, 47 -60

[10] Harris L., 1967. The optical properties of metal blocks and carbon blacks, The Eppley Foundation for Research Monograph, Series No. 1.

[11] Heaton H.S., Reynolds, We, and Kays W.M., 1964. Heat transfer in annular passages. Simultaneous development of velocity and temperature fields in laminar flow. Int J Heat Mass Transfer 7, 763-81.

[12] Hegazy NA, 2000. Thermohydraulic performance of air heating solar collectors with variable width, flat absorber plates, Energy Convers Manage 41, 1361 - 1378

[13] Hikmet E. 2008. Experimental Energy and Exergy Analysis of a Double-Flow Solar Air Heater Having Different Obstacles on Absorber Plates, Building and Environment 43, 1046-1054

[14] Hitesh N Panchal. Nirav Soni, Mitul Prajapti, Jignesh Prajapti, Parth Shah, Umang Soni and Diptesh Patel, 2011. Experimental investigation on double pass air heater with corrugated absorber plate and amul cool aluminum cans. International Journal of Advanced Engineering Technology. Vol. II (III), 324 – 328

[15] Ho C.D., Yeh H.M., Cheng T.W., Chen T.C. and Wang R.C., 2009. The Influences of Recycle on Performance of Baffled Double-Pass Flat-Plate Solar Air Heaters with Internal Fins Attached. Applied Energy 86, 1470-1478

[16] Ho C.D., Yeh H.M. and Wang R.C., 2005. Heat-transfer Enhancement in Double-Pass Flat-Plate Solar Air Heaters with Recycle. Energy 30, 2796-2817

[17] Hollands K.G.T and lynkaran K., 1993. Analytical model for the thermal conductance of compound honeycomb transparent insulation, with experimental validation. Solar Energy 51 (3), 223-227

[18] Hollands K.G.T. and lynkaran K., 1985. Proposal for a compound honeycomb collector. Solar Energy 34, 309-316.

[19] Hollands K.G.T. and Shewen E.C. 1991. Optimization of flow passage geometry for air-handling, plate type solar collectors. Journal of Solar Energy Engineering 103, 323 – 330

[20] Hottel H.C. and Woertz B.B., 1942. Performance of flat plate solar heater collectors, Trans. ASME 64,91-104.

[21] Hsieh, J. S., 1986. Solar Energy Engineering, Prentice Hall Inc. New Jersey

[22] TBEF Power (http://www.india-opportunities.es/archivos/publicaciones/ Power-January-2016.pdf) (PDF). IBEF. Retrieved 28 October 2016.

[23] India can achieve 1,650 billion units of electricity next year, Piyush Goyal (http://economictimes.indiatimes.com/industry/energy/power/india-canachieve -1-65 -billion-units-of-electricity-next-yearpiyushgoyal/ articleshow /53103685. cms). Retrieved 9 July 2016

